Materials Research Express

PAPER

Wear behavior of glass microballoon based closed cell foam

Materials Research Express

PAPER

Wear behavior of glass microballoon based closed cell foam

Mrityunjay Doddamani
Lightweight Materials Laboratory, Mechanical Engineering, National Institute of Technology Karnataka, Surathkal, 575025, India
E-mail: mrdoddamani@nitk.edu.in

Keywords: syntactic foam, glass microballoon, wear

RECEIVED
14 June 2019

REVISED
10 August 2019

ACCEPTED FOR PUBLICATION
13 September 2019

PUBLISHED
27 September 2019

Abstract

Present work deals with dry sliding wear response of hollow glass microballoons reinforced lightweight epoxy syntactic (closed cell) foams using a pin on disc apparatus. Influence of glass microballoons content on wear behavior of hollow glass microballoons/epoxy foams in dry sliding mode is investigated. Effects of sliding velocity (1 and 3 m s^{-1}), normal load (30–50 N), sliding distance (1 and 3 km) and glass microballoons content (20, 40 and 60 volume%) are investigated. The rate of wear declines with increasing glass microballoons content and sliding distance. Syntactic foams with perfectly spherical glass microballoons exhibit enhanced resistance to wear as compared to neat resin samples due to better constituents compatibility. Specific wear rate shows noticeably decreasing magnitude with higher applied load. Decrease in frictional coefficient is observed with higher filler loadings. Lowest wear rate of 1.6 mm^3 km^{-1} is noted for sliding velocity and load of 3 m s^{-1} and 50 N respectively with 60 filler volume %. Low wear values with higher glass microballoon loadings support the feasibility of utilizing such foams in wear-prone applications in weight sensitive structures. Wear mechanisms are studied using scanning electron microscopy. Finally, property map is presented to compare the observed wear results with the existing studies available on dry sliding wear response.

Nomenclature

GMB	Glass microballoons
WMC	Wax containing microcapsules
ρ	Composite density (kg/m^3)
ρ^{th}	Density—Theoretical (kg/m^3)
ρ^{exp}	Density—Experimental (kg/m^3)
ϕ_V	% content of voids
V	Velocity in sliding mode (m/s)
W	Volume of wear
D	Sliding distance in mm
w_t	Rate of wear in mm^3/km
w_r	Resistance to wear in km/mm^3
w_s	Wear rate (specific) in mm^3/km-N
F	Force in N
μ	Frictional coefficient
F_T	Force - Tangential in N
F_N	Force - Normal in N

Introduction

Syntactic foams are lightweight polymer matrix composites offering better specific properties. These advanced materials offer lower density combined with higher strength and damage tolerance making them viable to be utilized in numerous applications of marine, transportation and aircraft structures [1, 2]. Syntactic foams are made by mixing microballoons in a resinous matrix. Polymer composites reveal exceptional friction and wear features and offer excellent resistance to corrosion. Wear and friction of surfaces sliding against each other initiate complex set of changes occurring at microscopic scales. Such changes are influenced by the constituents, geometry, topological features of the sliding surfaces and operating environment. Applications such as automotive brake linings have used friction materials made from syntactic foams [3]. Wear most frequently occurs phenomena in such applications demand innovation in technology and thrust for developing newer material system necessitates materials with enhanced properties for tribological applications [4, 5]. Wear behavior is dependent on the constituent materials, geometry, treating conditions, filler content etc Fly ash cenosphere is used as filler in the recent studies [6]. These naturally available cenospheres contain several flaws/defects in the form of surface defects, porosity within the shell and variable thickness in the wall [7]. These adversely affect the overall mechanical performance of the lightweight composites. Composites to be designed for structural applications incline to use GMBs of higher quality as fillers, owing to their better-expected properties. These perfectly shaped spherical microballoons provide numerous benefits as compared to irregularly shaped mineral fillers [8]. Syntactic foams reinforced with GMBs display exceptional properties of higher specific compression [9–11], thermal stability and low density [12–14].

Hollow particle filled composites can possess substantial changes in tribological response and wear behavior as compared with solid particulate composites. Fractional wear occurring from shearing of porous walls opens up void space enclosed inside the hollow particles. These void spaces enhance wear resistance by accumulating wear debris and offering smoother surface [15]. Detailed studies to understand the wear mechanisms in these engineered glass microballoons is essential and is greatly desired in weight sensitive structures. Imani *et al* [16] revealed improvement in wear resistance and a decrease in μ is attained by maintaining a proper ratio of silica nano particles and wax containing microcapsules (WMC). Specific wear rate reduces by a factor of 3 and μ by 10 for silica/WMC/epoxy composites. Reduction in wear of samples containing WMC is accredited to thin and continuous transfer film formation on the steel ball surface. Studies by Manakari *et al* [15] showed that the rate of wear increases with applied load whereas specific wear and coefficient of friction decreases. However, reverse trends are seen with the higher volume fraction of cenospheres. Nanometer size particles reduce the wear of composites. Applied load is the most influential parameter on the increase in wear and μ followed by fly ash content, the diameter of track and time [17]. Findings revealed that higher fly ash content decreases the severity in the wear loss. As sliding speed increases wear loss increases significantly for neat resin. Features of worn surface are fly ash content and sliding velocity dependent [18]. Singh and Siddhartha revealed that μ and specific values of composites with cenospheres decrease with higher load and sliding speed while it increases with higher sliding distances. Syntactic foam with 40 weight % cenosphere particles reveal better wear properties as compared to composites having 50 cenospheres weight % [19]. Even though there is extensive literature available on thermosetting foams, studies on the tribological response of engineered hollow glass microballoons reinforced composites is yet to be reported. Growing demand of these lightweight closed cell foams in aviation and transportation sectors requires detailed understanding in wear regime.

Present work aims to understand the role of engineered hollow particle filled composites on the wear mechanism and to investigate critical factors that assist in developing superior friction materials using Pin-on-Disk (PoD) apparatus. PoD device has been used widely to study the wear response of constituents intended to be utilized in brake devices in numerous transport fields under stable operating environments [20, 21]. Investigations of hollow glass microballoons filled foams must be studied to identify the use of utilizing such hollow particles in commonly used applications. In this study, higher levels of velocity, normal load, and sliding distances are selected that are generally experienced by structural members. Hollow glass particles by 20, 40 and 60 volume % are reinforced in the epoxy matrix. These microballoons have an average outer diameter of 53 μm and wall thickness of 0.716 μm. These microballoons during wear phenomenon are difficult to rupture owing to their perfectly spherical shape and higher crushing strength as compared to fly ash cenospheres [22]. Neat epoxy samples are also fabricated for comparison. The response of w_t, w_s and μ are investigated for different V, F and D. Worn surfaces microscopy is conducted to correlate the wear data. Finally results from the existing study and data extracted from the literature is presented in the form of a property map that might act a guide for industry experts and researchers to select appropriate compositions as per requirement.

Figure 1. Wear set-up.

Materials processing

Materials

Lapox (L-12) epoxy having a density of 1192 kg m^{-3} (matrix) is obtained from Atul, Valsad, Gujarat, India. GMB fillers of grade SID-200Z are procured from Trelleborg, USA having a density of 200 kg m^{-3}. Average diameter and radius ratio of the filler is reported in [22]. GMB fillers are used in the as-received condition.

Syntactic foam preparation

Glass microballoons by 20, 40 and 60 vol% [23, 24] are mixed in epoxy resin gradually to attain a uniform and consistent slurry. Slow stirring is adopted for dispersing fillers in the matrix. Consequently, the hardener is mixed by 10 weight% into the slurry prior to pouring in aluminum molds. Slabs are cured for 24 h and post-cured for 3 h at 90 °C. Epoxy slabs are cast under same operating conditions for comparative analysis. Samples are coded as EXX, where E denotes epoxy resin and XX represents filler in volume%. Samples are prepared according to the dimensions mentioned in ASTM G99–17 [24]. ASTM D792–13 [25] is used to compute the sample densities. ρth is estimated by,

$$\rho\text{th} = \rho_f V_f + \rho_m V_m \tag{1}$$

where m and f represent matrix and filler respectively.

Void content (ϕ_V) is calculated using [26],

$$\phi_V = \frac{(\rho\text{th} - \rho^{\text{exp}})}{\rho\text{th}} \tag{2}$$

Testing methodology

Wear test

Dry sliding wear test is performed under ambient environment using TR-20LF-PHM400-CHM600 series tribometer (DUCOM, Bangalore). Wear set-up is presented in figure 1. Superior damping ability and higher resistance to wear against different counter materials makes grey cast iron and steel appropriate materials for rotor discs in automotive brake devices due to their high hardness and thermal conductivity [27–29]. Thus, EN-31 disc is used with 62 HRC hardness for studying wear response of the prepared specimens. Experiments are performed on 120 mm track dia. with 159 and 477 rpm resembling sliding velocities of 1 and 3 m s^{-1} respectively. Parameters utilized in this work are listed in table 1. Subscripts a, b and c in V_a, F_b and D_c [30] signify corresponding parameter values. Two average nominal contact pressures, 0.21 and 0.35 MPa correspond to an applied load of 30 N and 50 N respectively are used in the present investigation to realize low and mild wear conditions in brakes wherein sliding velocity and contact pressure product ranges within 0.3 and 20 MPa m s^{-1}. For such low and mild wear conditions, contact temperature (average) is below 250 °C in real braking conditions [27]. Though binders like epoxy and phenolic resin have low heat resistance and degradation temperatures fall in the range of 250 °C–475 °C, onset of the main transformations involving resin decomposition are reported is post 265 °C [31]. The wear track width is maintained at 12 ± 0.01 mm. The surface roughness of the disc is maintained at 0.11 μm by polishing the disc prior to each test with SiC paper. The test is performed as mentioned in [25] by clamping the sample (12 × 12 × 25.4 mm) rigidly in the sample holding device. Average values of three samples tested are reported to ensure repeatability. Frictional forces and height losses are noted

Table 1. Chosen parameters for the present work [15, 32].

Material and test parameters		Output wear parameters
GMB content, (volume %)	0, 20, 40 & 60	w_t (mm^3/km)
Load, F (N)	30 and 50	w_s (mm^3/km-N)
Sliding velocity, V (m/s)	1 and 3	μ
Sliding distance, D (km) [33]	1 and 3	

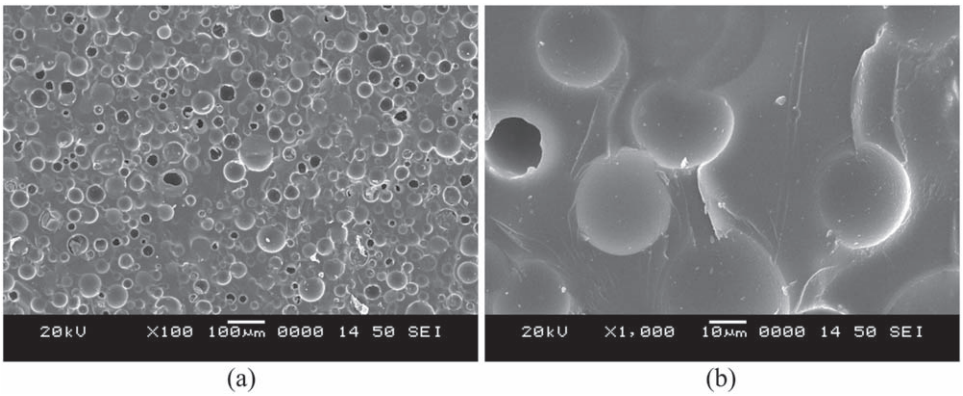

Figure 2. As prepared E60 at (a) lower and (b) higher magnifications.

during the test. Volume loss is computed using the cross-sectional area of the pin. Sliding speed and time lapse of the test are utilized to calculate the sliding distance. Wear rate (w_t) is determined by,

$$w_t = \frac{W_E - W_S}{d_E - d_s} \tag{3}$$

where subscripts E and S denotes end and start of steady-state wear.

Reciprocal of wear rate is represented as resistance to wear and is computed by,

$$w_t = w_t^{-1} \tag{4}$$

Load carrying capacity is accounted by specific wear rate (w_s) and is calculated using,

$$w_s = \frac{w_s}{F} \tag{5}$$

The coefficient of friction (μ) is given by,

$$\mu = \frac{F_T}{F_N} \tag{6}$$

Imaging

JEOL make (JSM 6380LA) scanning electron microscope (SEM) is used for micrography. Better conductivity is ensured by a gold coating of samples using JFC-1600 sputtering unit.

Result and discussions

Particle size analysis of GMB particles is reported in [22]. Micrographs of E60 sample at lower and higher magnification are presented in figure 2. Uniform distribution of GMB particles in an epoxy matrix with the minimal failure of particles is a challenge. Nevertheless, as cast micrographs of E60 (figure 2(a)) display evenly distributed GMBs in epoxy matrix justifying manual stirring technique to cast such lightweight syntactic foams. Few voids in the form of matrix porosity are also seen from figure 2(a). Manual stirring methodology results in such a matrix porosity. Such a porosity might help in accumulating wear debris resulting in enhanced wear resistance. Higher magnification of the E60 sample shows good bonding between the constituents (figure 2(b)). These perfectly spherical GMBs without any surface defects are likely to increase the foam performance due to good interfacial bonding. Table 2 presents density and weight saving potentials of the samples prepared. Sample

Table 2. Density and weight saving potential.

Details	ρ^{th} (kg/m^3)	ρ^{exp} (kg/m^3)	Φ_v (%)	Weight saving potential with E0
E0	1192	—	—	—
E20	1057.14	1027.60 ± 23.84	2.79	13.80
E40	842.10	816.20 ± 20.55	3.07	31.52
E60	649.64	619.80 ± 16.32	4.44	48.00

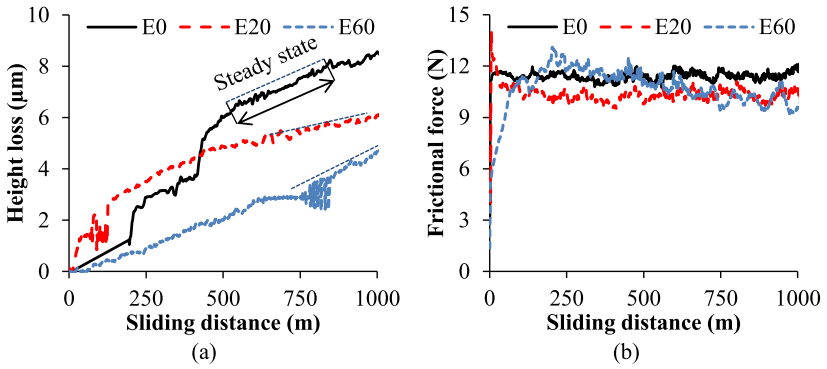

Figure 3. Representative plots of (a) loss in height and (b) frictional force w.r.t sliding distance.

density decreases with increasing GMB content. GMBs used in the current study are almost 6 times lower in density in comparison to epoxy resin. Thereby, higher number of GMBs in epoxy matrix reduces syntactic foam density significantly. Syntactic foam with 60 vol% of GMBs shows 48% lower density in comparison to neat epoxy. Such a significant reduction in density is very advantageous considering the need for lightweight materials in weight sensitive structures. Lower experimental density values in comparison with theoretical ones are primarily attributed to the presence of GMB particles in resin and partially owing to matrix porosity. Void volume % increases with higher filler loadings. Nonetheless, its well within 5% (table 2).

Figure 3 presents representative results of dry sliding wear on E0, E20, and E60 for $V_1F_{30}D_1$ test conditions. The loss in height (figure 3(a)) and frictional force (figure 3(b)) are plotted as a function of D. Wear of neat resin reaches a balanced state after an initial changeover period (figure 3(a)). E20 and E60 foams exhibit a similar trend, though the transient region is less prominent. Further, as observed in figure 3(a) loss in height for neat epoxy is higher as compared to that of syntactic foams at a sliding distance of 1000 meters indicates wear resistance enhancement due to GMB presence in the matrix resin. Frictional force in foams shows a decreasing trend with increasing time as compared to neat epoxy samples. As time progresses, frictional values achieve a steady state. For the same time interval, frictional values in E20 and E60 reduces as compared to neat resin exhibiting foams suitability in wear resistive scenarios. Fluctuations in figure 3(b) are more for neat epoxy samples as compared to the syntactic foams. Wear debris comes in contact with the sliding surface and disc resulting in more undulations leading to higher frictional force in case of neat epoxy specimens. In the case of syntactic foams, few glass microballoons fractures and the void space within open up during the initial wear test. These partially cut GMBs get filled with the wear debris (figure 3(b)). In due course of time, the number of new glass microballoons exposed for debris to get filled and wearing out of older microballoons balance each other, resulting in reduced frictional force as compared with the neat epoxy sample.

Wear rate (w_t)

The experimental values of w_t, w_s and μ for a V of 1 and 3 m s^{-1} are presented in tables 3 and 4 respectively. With increasing filler content, sliding distance and applied a normal load, w_t shows a decreasing trend. For all the test conditions, neat epoxy depicts the highest w_t as compared to all other foams. Higher applied normal load increases w_t for neat resin specimens while it decreases with higher GMB loading demonstrating the improvement attained by adding more filler in an epoxy matrix. Effects of process parameters on w_t are presented in figure 4. w_t decreases monotonically with GMB content for the given magnitude of the applied load, sliding distance and sliding velocity except for neat epoxy (figures 4(a) and (b)). These plots are beneficial for selecting an appropriate combination of factors that result in lower wear rates for a given application. Glass microballoons are hollow particles comprising of a thin hard shell. During wear, these glass microballoons of borosilicate glass offer resistance before finally getting fractured into multiple smaller fragments. These particles

Table 3. Experimentally computed w_t, w_s and μ.

V (m/s)	F (N)	D (m)	Material	w_t (mm^3/km)	w_s (mm^3/N-km)	μ
1	30	1	E0	7.5	0.255	0.432
			E20	7.4	0.251	0.387
			E40	6.8	0.231	0.369
			E60	4.1	0.139	0.351
		3	E0	5.4	0.183	0.383
			E20	4.6	0.156	0.373
			E40	4.4	0.150	0.342
			E60	4.2	0.143	0.325
	50	1	E0	10.1	0.206	0.420
			E20	6.9	0.141	0.432
			E40	5.9	0.12	0.405
			E60	2.7	0.055	0.362
		3	E0	10	0.204	0.410
			E20	6.2	0.126	0.406
			E40	5.1	0.104	0.379
			E60	2.4	0.049	0.363

Table 4. Experimentally computed w_t, w_s and μ.

V (m/s)	F (N)	D (m)	Material	w_t (mm^3/km)	w_s (mm^3/N-km)	μ
3	30	1	E0	9.5	0.323	0.557
			E20	6.8	0.231	0.514
			E40	6.5	0.221	0.518
			E60	4.2	0.143	0.487
		3	E0	6.1	0.207	0.544
			E20	5.3	0.18	0.494
			E40	5.1	0.173	0.485
			E60	4.2	0.143	0.440
	50	1	E0	13.9	0.283	0.646
			E20	4.6	0.094	0.560
			E40	3.9	0.08	0.478
			E60	2.8	0.057	0.482
		3	E0	7.1	0.145	0.578
			E20	4.4	0.09	0.555
			E40	2.6	0.053	0.563
			E60	1.6	0.033	0.443

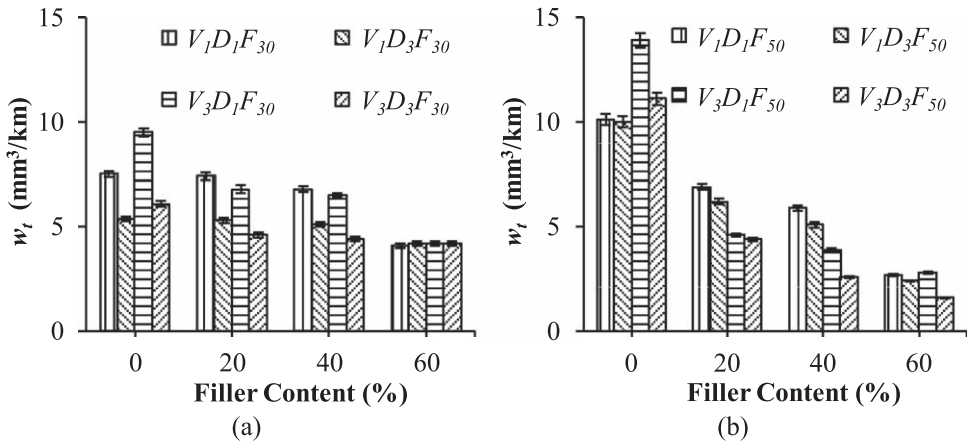

Figure 4. Plots of w_t for different filler contents, sliding velocities and distances (a) F_{30} and (b) F_{50}.

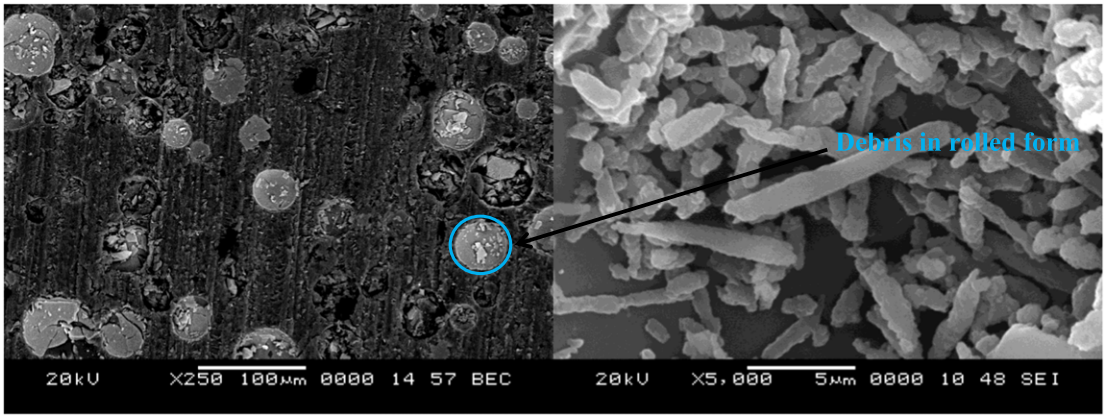

Figure 5. (a) Post wear test micrograph of E60 and (b) higher magnification micrograph of marked circle in (a).

with epoxy matrix form debris [34]. This debris accumulates within the fragmented hollow glass microballoons and in turn, lowers wear in foams. As the filler loading increases, availability of more number of hollow glass microballoons on the wear surface to accumulate wear debris decreases w_t significantly. Lower load (30 N) induces abrasive wear for syntactic foams due to wear debris inadequate compaction. In the case of the neat epoxy sample, more amount of wear debris is formed and subsequently create grooves leading to abrasive wear on the wear surface due to the absence of void space as in GMBs that aids for debris compaction. At a higher applied load of 50 N, w_t considerably increases for pure epoxy specimens and is attributed to higher frictional values attained at the interface of wear. w_t declines for GMB/epoxy composites due to GMBs resistance and their debris accommodative regions (figure 4). A similar observation is reported in [35] pertaining to the influence of normal applied load on w_t.

Surface morphology of neat epoxy samples without filler gets severely strained to create undulations on the wear surface forming wear debris. Higher applied load leads to debris adherance to the disc. On the contrary, most of the wear debris in GMB/epoxy foams accumulate at the craters of fragmented glass microballoon particles. The remaining wear debris facilitates in creating good plastic flow and relatively smoother surface at the sample-disc interface. Higher filler loading further reduces w_t owing to more space for wear debris accumulation. Micrographs of representative specimens at higher operating conditions post wear test with 60 vol.% of GMB in epoxy resin are presented in figure 5. Wear debris are seen on the surface of the sample as well as void spaces of GMB particles (figure 5(a)). Micrograph of wear debris filled GMB particle captured at high magnification reveals debris in circular rod form (figure 5(b)). These circular cross-section of wear debris is owing to the better compaction achieved with higher applied load and velocity. Such compacted wear debris reduce the fluctuations effectively resulting in significant enhancement of syntactic foams wear resistance.

Specific wear rate (w_s)

Standardizing observed w_t values with load provides more clarity in the observed trends. w_s as a function of GMB content is graphed in figures 6(a) and (b) for varying the sliding distance and applied force respectively at constant sliding velocity. It is seen that w_s reduces with increasing D and filler loading (figure 6). Although the w_t is maximum at an applied load of 50 N (figure 4(b)), normalization shows that w_s is lower at the same applied load for all the syntactic foams signifying superior wear resistance at higher applied load [36, 37]. Such scenarios make these GMB filled syntactic foams very suitable for wear-prone scenario. Trends observed with varying sliding distance and GMB content are similar to that observed for wear rate. Further, trends observed with higher sliding velocity are also on similar observations (figure 6(b)).

E60 reveal minimum w_s for all the test conditions as observed from figure 6. It is also observed that higher GMB content is desired for both w_t and w_s to be lower. Higher GMB content on the worn surface results in greater contact space enhancing wear resistance for E60 compared to all the other samples. E60 foam sample reveals minimum w_s of 0.033 $mm^3\ N^{-1}$-km while highest w_s of 0.323 $mm^3\ N^{-1}$-km is noted for the pure epoxy specimen. Transfer film formation on the wear surface owing to the influence of higher V and F is crucial in decreasing w_s [15].

Frictional coefficient (μ)

Figure 7 presents μ variation for different filler contents, sliding velocities and distances. Compared to all other foams, pure epoxy exhibits maximum μ. μ decreases with increasing D. Surfaces of both epoxy and GMBs

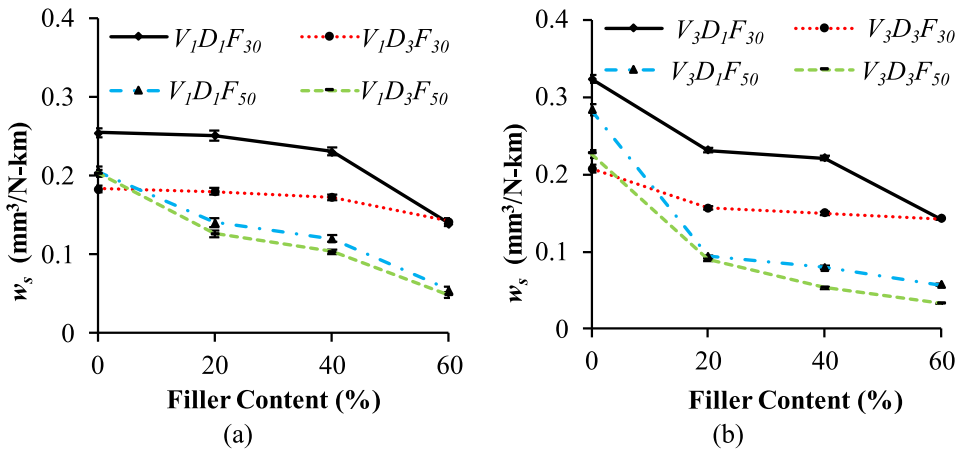

Figure 6. Plots of w_s for different filler contents, sliding velocities and distances (a) F_{30} and (b) F_{50}.

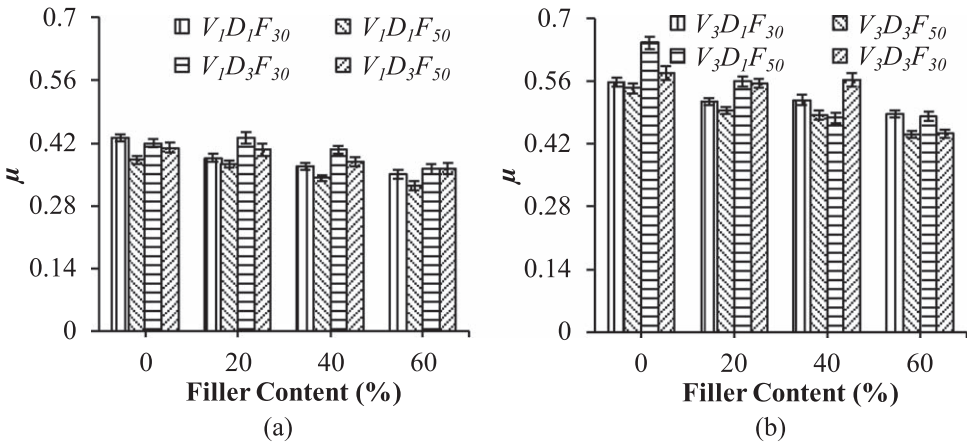

Figure 7. Frictional coefficient w.r.t. filler loading for (a) V_1 and (b) V_3 sliding velocities.

smoothen with an increase in sliding distance resulting in reduced μ values. Increase in sliding distance results in a change of surface chemistry, contact area and surface roughness [38]. It is also observed from figure 7(a) that μ reduces with increasing filler loadings. As the GMB content increases, chances of broken GMBs approaching the counter face are higher, thereby causing small data variations that lead to low roughness and μ values. Variation of μ for higher velocity (3 m s^{-1}) is presented in figure 7(b). Increase in sliding velocity increases μ values (figure 7(b)) due to induction of high shear forces leading to a higher temperature at sample and disc interface. As a result, test specimens are subjected to higher thermal dispersion and the bonding between constituents deteriorates. Therefore, GMB particles are easily displaced and fragmented due to axial thrust and results in higher μ values. With the increased V, μ increases for all the syntactic foams whereas it shows a declining trend with higher sliding distance, filler content and applied load.

Wear surface analysis

Wear surface micrograph for a load of 30 N and sliding velocity of 1 m s^{-1} is presented in figure 8. Neat epoxy wear surface reveals shallow and fine abrasive grooves and craters along the sliding direction. These grooves indicate higher material removal from the surface due to abrasive action as seen from figure 8(a). For E20 samples due to shearing action, cenospheres get pulled alongside the sliding path and get subsequently fragmented to open up the void space built within. Wear debris constituting of matrix and cenosphere gets spread over the craters of fragmented GMBs and gets accommodated within the opened void space as seen from figure 8(b). Such scenarios reduce the wear of GMB filled composites. Although the wear of E20 reduces, a significant reduction cannot be attained owing to the dominance of matrix on wear response. Embedding more number of GMB particles into the matrix reduces the wear rate significantly owing to the higher resistance offered by the GMB particles, reduced matrix content and more space availability for debris accumulation (figure 8(c)) [15].

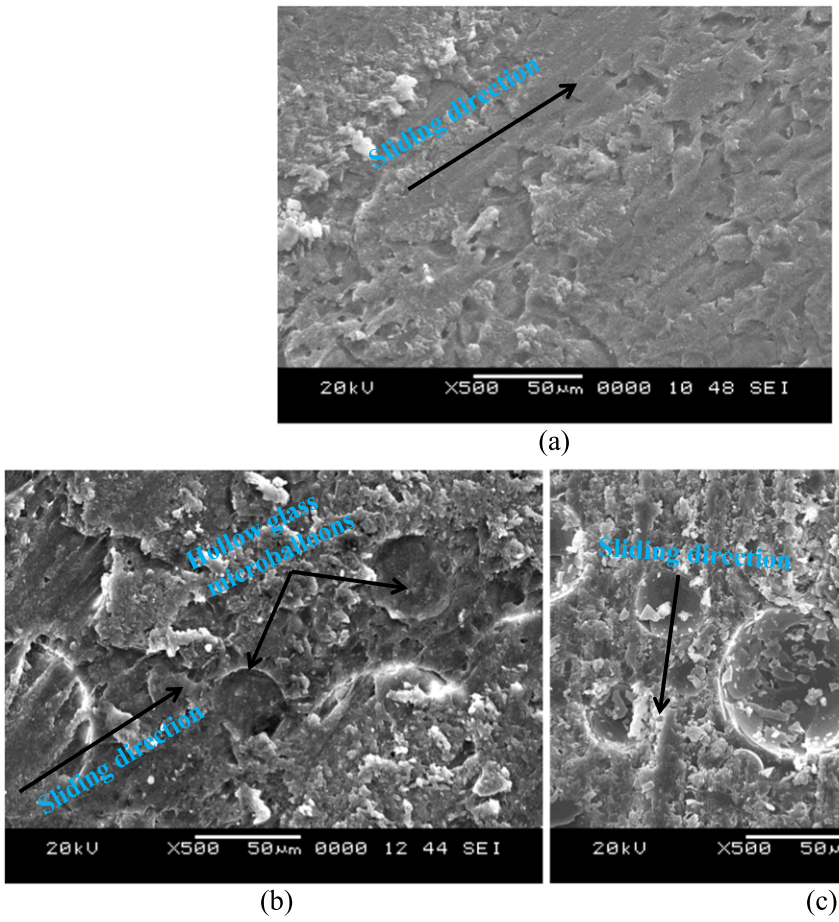

Figure 8. Post-test SEM of (a) E0 (b) E20 and (c) E60 at V_1F_{30}.

Figure 9 presents wear micrograph for V_3F_{50} condition. Higher F and V accelerates the probability of debris smearing along the worn path of neat epoxy samples resulting in higher material flow (figure 9(a)). Plucking marks can be visible on neat sample along the sliding direction indicating enhanced w_t. Wear micrographs of E20 and E60 are presented in figures 9(b) and (c) respectively. Wear debris is accumulated in the void space of GMBs and remaining debris gets spread over the surface (figure 9(b)). Compared to E20 at lower operating conditions (figure 8(b)), figure 9(b) reveals better compaction of wear debris owing to higher applied conditions. However, debris is not completely compacted due to higher matrix content at lower filler loading. Higher filler loading provides an opportunity for a lot of opened void spaces post GMB breakage leading to compacted debris (figure 9(c)) and transfer film formation on the wear surface resulting in adhesive wear [39]. Wear rate decreases considerably for E60 in comparison to E0. Higher V and F increase the probability of forming uniform transfer film resulting in enhanced wear resistance for E60 as compared to other samples. Furthermore, higher applied load stabilizes the surface asperities/severities exhibiting steadier w_t [15]. Additionally, hard shells of GMB particles resist wear and aid further w_t decline.

Property map

Property map is presented to show the effectiveness of the proposed material system with respect to the existing studies available on dry sliding wear response. These maps act as a guide and are useful for researchers and industrial practitioners in selecting the specific configuration based on the requirements. Information collected from the existing studies is compared with the results of the present work [15, 32, 40] (figure 10). High-density polymer composites reveal higher rates of wear as seen from the map. However, the benefits of hollow glass microballoons filled foams is clearly seen in figure 10. The density of all the syntactic foams prepared in the present work is observed to be significantly lower than other composites presented in the property map. The density of GMBs is 200 kg m^{-3}. Reinforcing higher content of these particles reduces the overall density of the composites substantially. E60 foam reveals almost 50% weight reduction compared to all other composites as evident from figure 10. Except for cenosphere/vinyl ester composites filled with 10 and 15 weight% of cenospheres, wear rate of hollow glass microballoon foams outperform all other composites. Property map indicates that GMB filled epoxy syntactic foams display much lower specific wear rates as compared to other

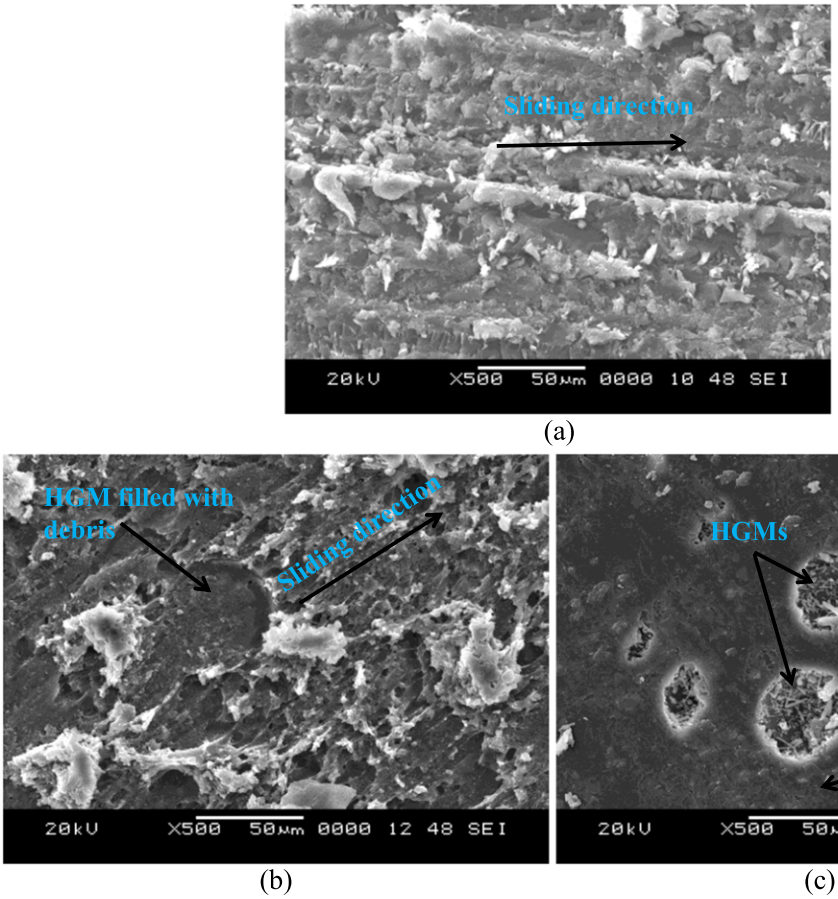

Figure 9. Post-test SEM of (a) E0 (b) E20 and (c) E60 at V_3F_{50}.

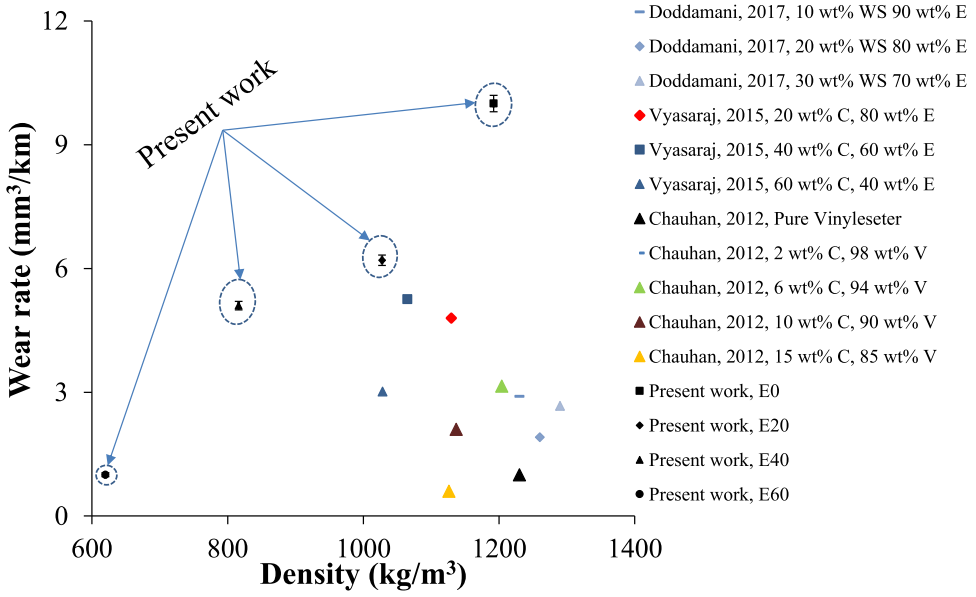

Figure 10. Rate of wear w.r.t composite density extracted from literature [15, 32, 40]. Note: WS—Walnut Shell, E—Epoxy, C—Cenosphere, V—Vinylester.

composites demonstrating the aptness of these foams in lightweight applications exposed to dry sliding wear conditions.

Conclusions

Wear response of hollow glass microballoons reinforced epoxy syntactic foams in dry sliding mode is investigated for varying velocity, sliding distance and applied load. Conclusions are summarised as below:

- Pure epoxy samples exhibit maximum wear for all the test conditions whereas the w_t decreases with increase in GMB content in the composites.
- Wear resistance of E20, E40 and E60 samples in comparison to pure epoxy samples increases by 60.36, 76.58 and 85.59% respectively.
- Higher applied for load show a significant decrease in specific wear of foams. E60 samples are best suited for wear applications.
- Frictional coefficient declines with higher sliding distance and GMB content.
- Higher w_t of neat epoxy is characterized by visible grooves along the sliding direction while the inclusion of GMBs reduces the wear considerably for E60 as compared to E20 at lower operating conditions.
- Wear rate decrease for foams is attributed to the availability of void space to accumulate wear debris. Abrasive wear mode is prominently observed.
- SEM for higher operating conditions exhibits adhesive wear mode prominently. Wear rate recorded for neat epoxy is high owing to higher material removal from the wear surface. Better compaction of wear debris in the void space of GMB particles leading to the formation of thin films is attributed to reduced wear of syntactic foams.
- Property map indicates that the GMB filled epoxy syntactic foams display significantly lower wear rates demonstrating the suitability of the developed foams in the present investigation for weight sensitive structures.

ORCID iDs

Mrityunjay Doddamani https://orcid.org/0000-0002-5537-9404

References

[1] Gupta N, Zeltmann S E, Shunmugasamy V C and Pinisetty D 2014 Applications of polymer matrix syntactic foams *JOM* **66** 245–54
[2] Jayavardhan M L, Bharath Kumar B R, Doddamani M, Singh A K, Zeltmann S E and Gupta N 2017 Development of glass microballoon/HDPE syntactic foams by compression molding *Composites Part B: Engineering.* **130** 119–31
[3] Luong D D, Strbik O M III, Hammond V H, Gupta N and Cho K 2013 Development of high performance lightweight aluminum alloy/SiC hollow sphere syntactic foams and compressive characterization at quasi-static and high strain rates *J. Alloys Compd.* **550** 412–22
[4] Singh A K, Patil B, Hoffmann N, Saltonstall B, Doddamani M and Gupta N 2018 Additive manufacturing of syntactic foams: I. Development, properties, and recycling potential of filaments *JOM* **70** 303–9
[5] Singh A K, Saltonstall B, Patil B, Hoffmann N, Doddamani M and Gupta N 2018 Additive manufacturing of syntactic foams: I. Specimen printing and mechanical property characterization *JOM* **70** 310–4
[6] Shahapurkar K, Chavan V B, Doddamani M and Kumar G C M 2018 Influence of surface modification on wear behavior of fly ash cenosphere/epoxy syntactic foam *Wear* **414-415** 327–40
[7] Doddamani M and Kulkarni S M 2011 Dynamic response of fly ash reinforced functionally graded rubber composite sandwiches - a Taguchi approach *International Journal of Engineering, Science and Technology* **3** 17
[8] Manakari V, Parande G, Doddamani M and Gupta M 2017 Enhancing the ignition, hardness and compressive response of magnesium by reinforcing with hollow glass microballoons *Materials* **10** 15
[9] Kim H S and Khamis M A 2001 Fracture and impact behaviours of hollow micro-sphere/epoxy resin composites *Composites Part A: Applied Science and Manufacturing* **32** 1311–7
[10] Kim H S and Plubrai P 2004 Manufacturing and failure mechanisms of syntactic foam under compression⋆ *Composites Part A: Applied Science and Manufacturing* **35** 1009–15
[11] Gupta N and Nagorny R 2006 Tensile properties of glass microballoon-epoxy resin syntactic foams *J. Appl. Polym. Sci.* **102** 1254–61
[12] Calahorra A, Gara O and Kenig S 1987 Thin film parylene coating of three-phase syntactic foams *J. Cell. Plast.* **23** 383–98
[13] Bilow N and Sawko P M 1975 Coating processes for increasing the moisture resistance of polyurethane baffle material *J. Cell. Plast.* **11** 207–12
[14] Wouterson E M, Boey F Y C, Hu X and Wong S-C 2005 Specific properties and fracture toughness of syntactic foam: effect of foam microstructures *Compos. Sci. Technol.* **65** 1840–50

[15] Manakari V, Parande G, Doddamani M, Gaitonde V N, Siddhalingeshwar I G, Kishore V C S and Gupta N 2015 Dry sliding wear of epoxy/cenosphere syntactic foams *Tribol. Int.* **92** 425–38
[16] Imani A, Zhang H, Owais M, Zhao J, Chu P, Yang J and Zhang Z 2018 Wear and friction of epoxy based nanocomposites with silica nanoparticles and wax-containing microcapsules *Composites Part A: Applied Science and Manufacturing* **107** 607–15
[17] Pattanaik A, Satpathy M P and Mishra S C 2016 Dry sliding wear behavior of epoxy fly ash composite with Taguchi optimization *Engineering Science and Technology, an International Journal* **19** 710–6
[18] Barpanda P and Kulkarni S 2009 Sliding wear behavior of an epoxy system reinforced with particulate fly ash filler *Adv. Compos. Lett.* **18** 199–205
[19] Ray D and Gnanamoorthy R 2007 Friction and wear behavior of vinylester resin matrix composites filled with fly ash particles *J. Reinf. Plast. Compos.* **26** 5–13
[20] Federici M, Straffelini G and Gialanella S 2017 Pin-on-Disc testing of low-metallic friction material sliding against HVOF coated cast iron: modelling of the contact temperature evolution *Tribol. Lett.* **65** 121
[21] Rashid B, Leman Z, Jawaid M, Ghazali M J, Ishak M R and Abdelgnei M A 2017 Dry sliding wear behavior of untreated and treated sugar palm fiber filled phenolic composites using factorial technique *Wear* **380-381** 26–35
[22] Jayavardhan M L, Bharath Kumar B R, Doddamani M, Singh A K, Zeltmann S E and Gupta N 2017 Development of glass microballoon/HDPE syntactic foams by compression molding *Composites Part B: Engineering* **130** 119–31
[23] Gupta N, Gupta S K and Mueller B J 2008 Analysis of a functionally graded particulate composite under flexural loading conditions *Materials Science and Engineering: A* **485** 439–47
[24] Doddamani M, Kishore V C, Shunmugasamy N, Gupta and Vijayakumar H B 2015 Compressive and flexural properties of functionally graded fly ash cenosphere–epoxy resin syntactic foams *Polym. Compos.* **36** 685–93
[25] Hossain M M and Shivakumar K 2011 Compression fatigue performance of a fire resistant syntactic foam *Compos. Struct.* **94** 290–8
[26] Shahapurkar K, Garcia C D, Doddamani M, Mohan Kumar G C and Prabhakar P 2018 Compressive behavior of cenosphere/epoxy syntactic foams in arctic conditions *Composites Part B: Engineering* **135** 253–62
[27] Straffelini G, Verma P C, Metinoz I, Ciudin R, Perricone G and Gialanella S 2016 Wear behavior of a low metallic friction material dry sliding against a cast iron disc: role of the heat-treatment of the disc *Wear* **348-349** 10–6
[28] Straffelini G and Maines L 2013 The relationship between wear of semimetallic friction materials and pearlitic cast iron in dry sliding *Wear* **307** 75–80
[29] Parsons F E 2000 Wet Disc BrakeUS Patent 6119828Geelong West, Australia
[30] Matsunaga T, Kim J K, Hardcastle S and Rohatgi P K 2002 Crystallinity and selected properties of fly ash particles *Materials Science and Engineering: A* **325** 333–43
[31] Verma P C, Ciudin R, Bonfanti A, Aswath P, Straffelini G and Gialanella S 2016 Role of the friction layer in the high-temperature pin-on-disc study of a brake material *Wear* **346-347** 56–65
[32] Doddamani M, Parande G, Manakari V, Siddhalingeshwar I, Gaitonde V and Gupta N 2017 Wear response of walnut-shell-reinforced epoxy composites *Materials Performance and Characterization* **6** 25
[33] Kowsari E and Mallakmohamadi M 2012 Electrospun PAN nanofiber process control by ionic liquids and electromagnetic wave absorbing properties *Mater. Lett.* **79** 7–10
[34] Mondal D P, Das S and Jha N 2009 Dry sliding wear behaviour of aluminum syntactic foam *Mater. Des.* **30** 2563–8
[35] Kanchanomai C, Noraphaiphipaksa N and Mutoh Y 2011 Wear characteristic of epoxy resin filled with crushed-silica particles *Composites Part B: Engineering* **42** 1446–52
[36] Ghazali M J, Rainforth W M and Jones H 2005 Dry sliding wear behaviour of some wrought, rapidly solidified powder metallurgy aluminium alloys *Wear* **259** 490–500
[37] Shalwan A and Yousif B F 2014 Influence of date palm fibre and graphite filler on mechanical and wear characteristics of epoxy composites *Mater. Des.* **59** 264–73
[38] Rao R N and Das S 2011 Effect of sliding distance on the wear and friction behavior of as cast and heat-treated Al–SiCp composites *Mater. Des.* **32** 3051–8
[39] Kato K 2000 Wear in relation to friction — a review *Wear* **241** 151–7
[40] Chauhan S R and Thakur S 2013 Effects of particle size, particle loading and sliding distance on the friction and wear properties of cenosphere particulate filled vinylester composites *Mater. Des.* **51** 398–408